

Full length article

Theory of twin strengthening in fcc high entropy alloys

R.E. Kubilay*, W.A. Curtin

Laboratory for Multiscale Mechanics Modeling, Institute of Mechanical Engineering, École Polytechnique Fédérale de Lausanne, Lausanne CH-1015, Switzerland

ARTICLE INFO

Article history:

Received 16 November 2020

Revised 11 May 2021

Accepted 17 June 2021

Available online 24 June 2021

Keywords:

Twinning

Solute strengthening

Random alloys

ABSTRACT

Twinning in fcc High Entropy Alloys (HEAs) has been implicated as a possible mechanism for hardening that enables enhanced ductility. Here, a theory for the twinning stress is developed analogous to recent theories for yield stress. Specifically, the stress to move a twin dislocation, i.e. an fcc partial dislocation moving along a pre-existing twin boundary, through a random multicomponent alloy is determined. A reduced elasticity theory is then introduced in which atoms interact with the twin dislocation pressure field and the twin boundary. The theory is applied to NiCoCr using results from both interatomic potentials and elasticity theory. Results are also used to predict the increased stress for the motion of (i) a single partial dislocation leaving a trailing stacking fault and (ii) adjacent partial dislocations involved in twin nucleation. Increased strength is predicted for all processes involved in the nucleation and growth of fcc twins. Comparison to single-crystal experiments at room temperature then suggests that twinning is controlled by twin nucleation, with reasonable quantitative agreement. When solute/fault interactions are neglected, the theory shows that twinning and lattice flow stresses are related. The theory also provides insight into how other dilute solute additions could suppress twinning, as found experimentally.

© 2021 The Author(s). Published by Elsevier Ltd on behalf of Acta Materialia Inc. This is an open access article under the CC BY license (<http://creativecommons.org/licenses/by/4.0/>)

1. Introduction

Various fcc High Entropy Alloys (HEAs) have shown excellent mechanical properties, especially a combination of high strength and high ductility [1–5]. The origins of the high strength are well understood in terms of solid-solution strengthening [6]. All of the N elemental components in an HEA act as “solutes” and dislocations face high energy barriers as they move through the field of solutes. Thus, although each solute may have a small interaction with the dislocation, every atom contributes to the strengthening and so the alloys have a solute concentration of 100%. The origins of the high ductility, and associated high fracture toughness, are less-well understood. The CoCrFeMnNi and CoCrNi alloys show a plateau in work hardening that delays the onset of ductile necking according to the Considère criterion. It has been suggested that this plateau is due to observed twinning that locally hardens the microstructure in regions that might otherwise serve to initiate softening. High ductility may not require twinning however, as found in NiCoV [7] and in NiCoCr with dilute Al and Ti additions [8], but an understanding of twinning in fcc HEAs remains valuable since it is important to control all possible deformation mechanisms of an alloy.

Twinning in fcc elemental metals and dilute alloys is generally correlated with the stable stacking fault energy. In an elemental metal, there are three relevant processes as shown schematically in Fig. 1. The first process (Fig. 1a) is the motion of a single partial dislocation of Burgers vector b_p through the lattice, leaving behind a trailing stacking fault of energy γ_{SF} . The shear stress to move the partial dislocation is $\tau_p = \gamma_{SF}/b_p$. The second process is twin nucleation, which involves the motion of several adjacent partial dislocations through the lattice to create a twin nucleus. A mechanism involving lattice dislocation reactions to create a two-layer nucleus was recently proposed by Rao [9] (Fig. 1b), and the twin nucleation stress is then the stress to move the two partials through the material as shown in Fig. 1, with $\tau_{t,nuc} = 2\gamma_{twin}/2b_p$ where γ_{twin} is the twin boundary energy and with two new twin boundaries being formed during glide. A mechanism of Mahajan [10] involving three partial dislocations leads to a twinning stress of $\tau_{t,nuc} = 2\gamma_{twin}/3b_p$. After nucleation, twin growth is envisioned to occur easily when lattice dislocations impinge on the twin nucleus and dissociate into pairs of twinning dislocations. The twin thickens by the motion of the twin dislocations along the twin boundary (Fig. 1c) [11–13]. The stress to grow the twin is then negligible, assuming no inherent Peierls stress for motion of the twin along the twin boundary. Twin growth is then controlled by the stress required to move the lattice dislocations to the twin boundary.

* Corresponding author.

E-mail address: recep.kubilay@epfl.ch (R.E. Kubilay).

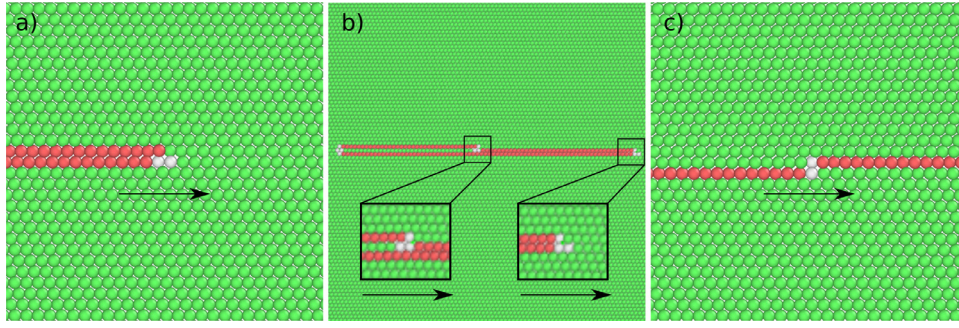


Fig. 1. a) Single partial dislocation moving through the lattice, with a trailing stacking fault. b) Two-layer twin nucleus proposed by Rao et. al. with a pinned structure on the left and two moving partial dislocations on the right. c) A twin dislocation moving along the twin boundary causing thickening of the twin. Arrows show the direction of dislocation glide. Atoms are colored according to Common Neighbor Analysis using OVITO [14] with green for fcc, red for hcp, white for others, enabling easy visualization of the faults and dislocation cores. (For interpretation of the references to color in this figure legend, the reader is referred to the web version of this article.)

Experimentally, there are widely varying reports of the twinning stress in the medium entropy alloy NiCoCr and the Cantor alloy CoCrFeMnNi. In single-crystal NiCoCr, Uzer et al. report a room-temperature twin strength of 78 ± 5 MPa [15]. In contrast, Laplanche et al. [16] estimated the twin strength from polycrystalline experiments as 273 ± 18 MPa at $T=77$ K and 241 ± 14 MPa at $T=293$ K, the latter far higher than the value of Uzer et al. With the common approximation that $\gamma_{twin} = 0.5\gamma_{SF}$, the twin nucleation strengths in NiCoCr based on the models discussed above are, using the reported value $\gamma_{SF} = 22$ mJ/m² [16], $\tau_{t,nuc} \approx 51$ and 76 MPa. These values are comparable to the values of Uzer et al. but disregard solute strengthening effects. The large difference between existing experiments and the absence effects of alloying, beyond their role in modifying the average stacking and twinning fault energies, motivates a study of the “solute strengthening” contribution to the twinning stress in random alloys.

Specifically, in a random alloy, the partial dislocations in all cases shown in Fig. 1 above must move through the random field of solutes. This imparts a solute strengthening contribution to all of the mechanisms shown in Fig. 1. That is, the strengths for the three processes become

$$\tau_p = \tau_p^{SS}(T, \dot{\epsilon}) + \gamma_{SF}/b_p \quad (1a)$$

$$\tau_{t,nuc} = \tau_{nuc}^{SS}(T, \dot{\epsilon}) + \gamma_{SF}/nb_p \quad (1b)$$

$$\tau_{t,growth} = \tau_{growth}^{SS}(T, \dot{\epsilon}) \quad (1c)$$

where $n = 2, 3$ for the Rao and Mahajan models, respectively. These contributions τ^{SS} to the strengthening, which are similar to the solute strengthening of full dislocations that controls the bulk material yield strength, have not been considered to date. Here, we develop the theory for the stress $\tau_{t,growth}$ for motion of a partial dislocation along the pre-existing twin boundary (Fig. 1c). We then subsequently argue that $\tau_p^{SS} \approx \tau_{nuc}^{SS} \approx \tau_{t,growth} = \tau_{growth}^{SS}$ and consider the additional cases shown in Fig. 1a,b. We apply our analysis to the case of NiCoCr, and we are able to rationalize the results of Uzer et al. We then extend the analysis to consider additional dilute solute additions, which increase the twinning stress relative to the lattice yield stress, corresponding to a relative suppression of twinning.

The general problem is similar to that for a lattice dislocation, where the yield strength of many HEAs has been accurately predicted [6,17,18] based on a theory for “solute strengthening” in a random alloy [6]. The main difference in the process of twin growth (Fig. 1c) is that glide of the twinning dislocation shifts the plane of the trailing twin boundary - this is the twin thickening mechanism - and so the theory must include this phenomenon. A

similar application of the theory was made to examine twinning in dilute hcp Mg alloys, which differ quantitatively from the fcc twin case because the hcp twin Burgers vector is very small and the solute/hcp-twin-boundary interaction energies are rather large [11]. For fcc twinning, we predict that the twin partial is strengthened significantly in the random alloy due mainly to the elastic interactions of the twin dislocation with the solutes. The interactions of the solutes with the twin boundary are calculated to be -3.19 , -2.74 and 6.44 meV for Ni, Co and Cr, respectively. They are small enough so that the shifting of the twin boundary plane during twin growth is not significant. The predicted twin growth strength of NiCoCr at room temperature is 38–56 MPa, somewhat lower than the experiments of Uzer et al. This result suggests that twinning is nucleation controlled. Applying the theory to twin nucleation (Fig. 1b), as indicated in Eqs. (1a)–(1b) above, brings theory and experiment into some agreement.

The remainder of this paper is organized as follows. In Section 2, we present the general theory for the twin growth mechanism (Fig. 1c). In Section 3, the theory is applied to NiCoCr, extended to twin nucleation mechanisms (Figures 1a,b), and compared to experiments. Section 4 presents further analysis and implications of the model, while Section 5 summarizes our results.

2. Theory

We follow the general analyses presented in Varenne et al. [6,19] and refer readers to these papers for more details. We consider an N -component random fcc HEA with concentration c_n of the n^{th} element ($\sum_{n=1}^N c_n = 1$). The alloy has an average reference material possessing all the average properties of the real alloy: lattice constant a , elastic constants $\{C_{ij}\}$, and stable/unstable stacking fault and twinning energies, all of which depend on the average alloy composition. Note specifically that the average effects of alloying on the fault energies are accounted for automatically.

We study the edge twin (fcc partial) dislocation lying on a pre-existing twin boundary as shown in Fig. 2a. The edge partial is expected to have the highest strengthening and thus control the motion of a twin dislocation loop as it expands along a twin boundary. The edge twin partial structure is common across all fcc materials although the precise atomic positions in the very core of the twin boundary may vary. Strengthening of the twin dislocation is due to the totality of interaction energies between the solutes and the twin dislocation as it glides along the twin boundary. The interaction energy for a solute of type n at position (x_i, y_j, z_k) relative to the center of a straight twin dislocation lying along z is denoted as $U^n(x_i, y_j, z_k)$. This energy has contributions from the elastic interaction between the solute misfit volume and the dislocation pressure field (Fig. 2b), the solute/twin boundary interactions, and additional possible “chemical” or inelastic energies for

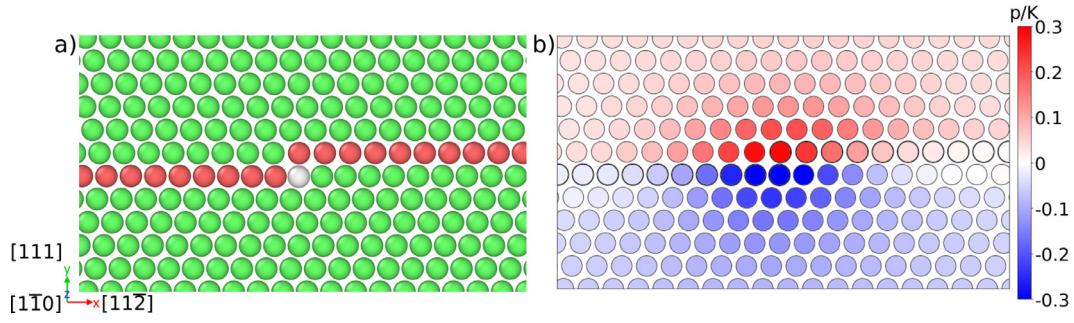


Fig. 2. a) Atomic configuration of a pure edge twin dislocation lying on the twin boundary. b) Normalized pressure field along the twin boundary and around the twin dislocation in a model NiCoCr alloy.

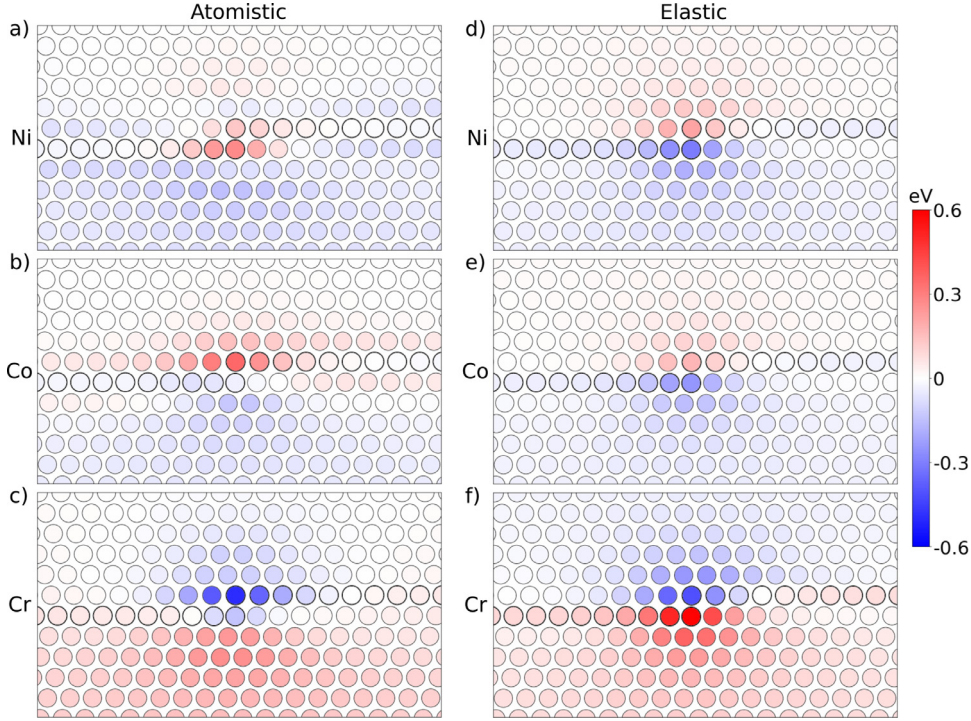


Fig. 3. Interaction energies of Ni, Co and Cr with the edge twin dislocation as obtained from the interatomic potential of Li et al. [21] and the elasticity approximation. The configurations were obtained using LAMMPS [22].

solutes in the very core of the twin dislocation. **Figures 3** show the interaction energies for Ni, Co, and Cr in the average NiCoCr alloy [20] as described by the interatomic potential of Li et al. [21]; this potential has accurate elastic constants for NiCoCr and accurate misfit volumes for Ni, Co, and Cr in NiCoCr and so is suitable for the present study.

The random distribution of solutes in a random alloy gives rise to local fluctuations in solute concentrations. An initial straight twin dislocation thus becomes wavy: it is attracted to energetically-favorable fluctuations and repelled by energetically-unfavorable fluctuations. The relevant quantity is the potential energy change of a straight dislocation segment of length ζ at initial position $x = 0$ gliding over a distance w ,

$$\Delta U_{\text{tot}}(\zeta, w) = \sum_{i,j,k} \sum_n s_{ijk}^n [U^n(x_i - w, y_j, z_k) - U^n(x_i, y_j, z_k)] \quad (2)$$

where $s_{ijk}^n = 1$ if a type- n solute is at position (x_i, y_j, z_k) and 0 otherwise. The typical potential energy decrease when the dislocation segment ζ moves into a region of *favorable* solute fluctuations is given by the standard deviation of the potential energy change

$\sigma_{\Delta U_{\text{tot}}}(\zeta, w)$ that can be derived as

$$\sigma_{\Delta U_{\text{tot}}}(\zeta, w) = \left(\frac{\zeta}{\sqrt{3}b} \right)^{1/2} \Delta \tilde{E}_p(w) \quad (3)$$

$$\text{with } \Delta \tilde{E}_p(w) = \left[\sum_{i,j} \sum_n c_n (U^n(x_i - w, y_j) - U^n(x_i, y_j))^2 \right]^{1/2} \quad (4)$$

$\Delta \tilde{E}_p(w)$ is the key quantity for strengthening in the theory. These results apply generally [6], and are not specific to the twin boundary; only the actual contributions to $U^n(x_i, y_j, z_k)$ depend on the twin geometry.

A long straight twin dislocation of length L then reduces its total energy by adopting a wavy configuration over some characteristic length ζ and amplitude w so as to reside everywhere in regions of favorable fluctuations. However, there is an energy cost to create the longer total dislocation line length that is $\Delta E_{\text{LT}}(\zeta, w) = \Gamma w^2 / 2\zeta$ where Γ is the twin dislocation line tension in the average alloy matrix. The actual wavy configuration minimizes the total

energy

$$\Delta E_{tot} = \left[\Gamma \frac{w^2}{2\zeta} - \left(\frac{\zeta}{\sqrt{3}b} \right)^{1/3} \Delta \tilde{E}_p(w) \right] \left(\frac{L}{2\zeta} \right) \quad (5)$$

versus both ζ and w , leading to energy-minimizing characteristic scales ζ_c and w_c . The minimization with respect to ζ can be performed analytically but the subsequent minimization with respect to w must be done numerically. In this wavy configuration, segments of length ζ_c sit in potential energy minimum with a typical energy barrier ΔE_b proportional to $\Delta \tilde{E}_p(w_c)$ lying at a typical glide distance w_c from the minimum. To glide, the twin dislocation must overcome ΔE_b by a combination of thermal activation and the work $-\tau b \zeta_c x$ done by an applied resolved stress τ on the ζ_c segment as it glides a distance x relative to the minimum energy position. The resulting energy barrier and zero-temperature flow stress τ_{y0} , i.e. the stress at which the energy barrier vanishes, are then

$$\Delta E_b = 1.22 \left(\frac{w_c^2 \Gamma \Delta \tilde{E}_p^2(w_c)}{b} \right)^{1/3} \quad (6)$$

$$\tau_{y0} = \frac{\pi}{2} \frac{\Delta E_b}{b \zeta_c(w_c) w_c} = 1.01 \left(\frac{\Delta \tilde{E}_p^4(w_c)}{\Gamma b^5 w_c^5} \right)^{1/3} \quad (7)$$

At stresses $\tau < \tau_{y0}$, the plastic strain-rate is controlled by the rate of thermally activated glide of the dislocation segments over the stress-dependent energy barrier according to an Arrhenius model [23,24]. The finite-temperature, finite strain-rate flow stress $\tau_{t.growth}^{SS}(T, \dot{\epsilon})$ for twin partial motion along the twin boundary can then be obtained. There are low and high temperature regimes [25,26] but here, for simplicity, we use an interpolated form introduced in Ref. [27] that is accurate over a wide temperature range as

$$\tau_{t.growth}^{SS}(T, \dot{\epsilon}) = \tau_{y0} \exp \left[-\frac{1}{0.55} \left(\frac{kT}{\Delta E_b} \ln \frac{\dot{\epsilon}_0}{\dot{\epsilon}} \right)^{0.91} \right] \quad (8)$$

The twin strength is thus determined solely by the solute/twin-dislocation and solute/twin-boundary interaction energies and the twin dislocation Burgers vector and line tension. The structure of the theory is identical to the theory for full lattice dislocations [6].

The solute/twin interaction energies predicted by any approximate interatomic potential are not necessarily quantitatively accurate for the real material. And, even then, potentials are not available for most alloys of interest. So, to obtain insight and generality, we make a simplifying approximation for the solute/twin interaction energies. We represent the interaction energy as a sum of an elastic contribution from the twin dislocation pressure field and a solute/twin boundary interaction energy as $U_{el}^n(x_i, y_j, z_k) = -p(x_i, y_j) \Delta V_n + E_{n,twin}(x_i, y_j)$ where $p(x_i, y_j)$ is the pressure field around the twin dislocation, ΔV_n is the misfit volume of solute n in the bulk material, and $E_{n,twin}(x_i, y_j)$ is the solute/twin-boundary interaction energy in the absence of any twin dislocation. Since the reference for both ΔV_n and $E_{n,twin}$ is the average alloy [20], there are two sum rules, $\sum_n c_n \Delta V_n = 0$ and $\sum_n c_n E_{n,twin}(x_i, y_j) = 0$ (for all positions (x_i, y_j)), that must be satisfied for any alloy. Figure 3d,e,f show the misfit contribution $-p(x_i, y_j) \Delta V_n$ for Ni, Co, and Cr in the average NiCoCr alloy, showing that this contribution dominates the total interaction energy at most positions around the twin dislocation, but also with some differences relative to the full atomistic result using the same Ni-Co-Cr potential. Figures 3a,b,c show also that $E_{n,twin}(x_i, y_j)$, which can be seen clearly far from the twin dislocation, is non-negligible only for solutes lying on or just above/below the twin boundary. The contributions of $E_{n,twin}(x_i, y_j)$ for sites in the twin core, where the twin

boundary plane is shifting, cannot be cleanly separated from other core effects.

The twin boundary can have an intrinsic stress with pressure field $p_{twin}(x_i, y_j)$ in/around the twin boundary, as seen in Fig. 3d,e,f far from the twin core. If the solute/twin-boundary interaction energy is approximated only by the twin boundary pressure effect as $E_{n,twin} = -p_{twin}(x_i, y_j) \Delta V_n$, then Eq. (4) can be simplified to

$$\Delta \tilde{E}_p(w) = \left[\left(\sum_n c_n \Delta V_n^2 \right) \left(\sum_{i,j} (\Delta p_{ij}(w) + \Delta p_{ij,twin}(w))^2 \right) \right]^{1/2} \quad (9)$$

where $\Delta p_{ij}(w) = p(x_i - w, y_j) - p(x_i, y_j)$ and $\Delta p_{ij,twin}(w) = p_{twin}(x_i - w, y_j) - p_{twin}(x_i, y_j)$. In this reduced elastic case, the random effects of the solutes appear only through the quantity $\sum_n c_n \Delta V_n^2$. Furthermore, the dislocation plus twin pressure fields together correspond to the total pressure field. The form of $\Delta \tilde{E}_p(w)$ is then identical to that for the elasticity theory for lattice dislocations, differing only in the details of the total pressure field.

For specific solute/twin interaction energies $U^n(x_i, y_j)$, the minimization of Eq. (5) with respect to w is performed numerically. The minimized quantities are then inserted into Eqs. (6)–(8) to determine the twin strength in the alloy. In keeping with previous theory, the line tension is taken as $\Gamma = \mu_{110/111} b_p^2 / 8$ where $\mu_{110/111}$ is the alloy shear modulus for slip on the {111} plane in the <110> direction and the reference strain rate is $\dot{\epsilon}_0 = 10^4 \text{s}^{-1}$, consistent with previous work [6,28].

3. Twinning in NiCoCr

We now apply the theory outlined above for twin growth in NiCoCr. The interaction energies using the interatomic potential of Li et al. were shown in Fig. 3a,b,c. These potentials show solute/twin-boundary interactions in the twin plane and the planes just above and below the twin plane. The total pressure field as computed using the same interatomic potential and the individual solute misfit volumes for Ni, Co, and Cr in NiCoCr as measured by Yin et al. [29], combine to give the elasticity estimate for the interaction energies as shown in Fig. 3d,e,f. For the potential of Li et al., the differences between $E_{twin,n}$ and $-p_{twin} \Delta V_n$ along the twin boundary plane are quite small (compare Fig. 3a,b,c to d,e,f, respectively, away from the core region); this is not necessarily generally the case. The pressure field does not capture the interaction energies for solutes just off the twin boundary that are present when the full interatomic potential is used.

Figure 4a show the energies $\Delta E_{tot}(w)$ versus w for both atomistic and elasticity inputs. The behavior is similar for both cases, with both having a minimum at $w_c/1.5b_p = 4$. The atomistic energy at the minimum is less negative than for the elastic model, which leads to a lower strength and lower barrier. Recall that the atomistic input is not better than the elasticity model since the interatomic potentials do not necessarily accurately predict the solute/twin interaction energies in the core. Inserting the minimum total energy and minimum w_c into Eqs. (6)–(8) leads to the predictions of twin growth strength versus temperature as shown in Fig. 4b with $\mu_{110/111} = 78 \text{ GPa}$ [29] and $\dot{\epsilon} = 10^{-4} \text{s}^{-1}$. At room temperature, the predicted twin growth stress is 38 MPa for the atomistic model and 56 MPa for the elastic model. There is a strong temperature dependence in both cases, due to the thermally-activated nature of the process and the moderate energy barrier of 0.50 eV and 0.55 eV for atomistic and elastic models, respectively.

The predicted twin growth stresses are lower than the bulk lattice yield stress, reported to be 69 MPa by Uzer et al. and predicted to be 64 MPa by Yin et al. [29]. This indicates that twin growth would be controlled by the bulk lattice dislocation yield stress, which is the stress needed to move lattice dislocations that can

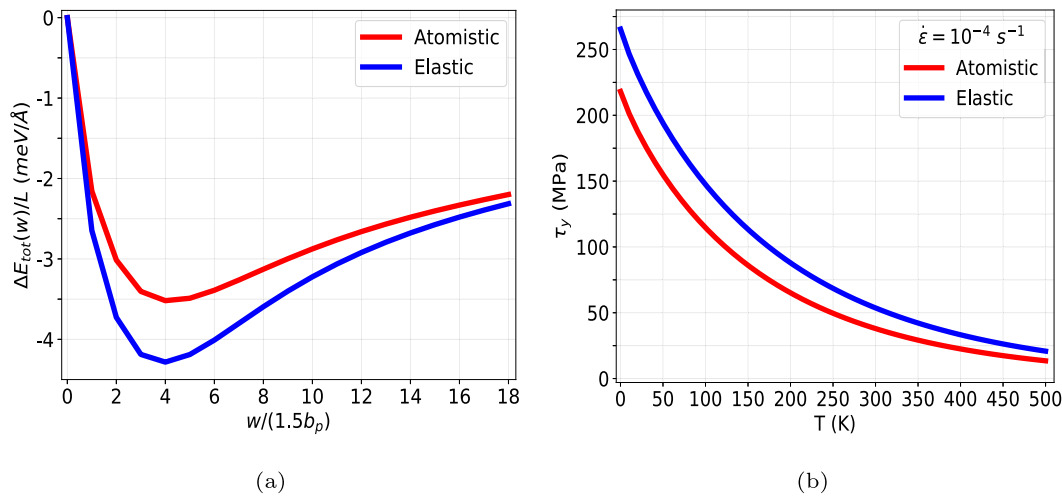


Fig. 4. a) $\Delta E_{tot}(w)/L$ versus w normalized with $1.5b_p$ for the atomistic and elastic cases. b) The twinning stress with respect to temperature for both cases.

then impinge and dissociate on the twin plane and lead to twin growth. The subsequent motion of the twin dislocations (Fig. 1c) would then occur easily since the (predicted) required stress is lower. Twinning is also observed to occur only after yield, but at somewhat higher stresses. These aspects suggest that twinning is controlled by nucleation (Fig. 1b) rather than growth. Furthermore, in the single-crystal experiments of Uzer et al., the Schmid factor for twinning is higher than that for slip ($m_t = 0.47$, $m_l = 0.41$ for the [110] orientation; $m_t = 0.31$, $m_l = 0.27$ for the [111] orientation), indicating that, at the same applied stress, twinning should be preferable to lattice dislocation motion. The observations then again suggest that twinning in NiCoCr is controlled by nucleation.

In the presence of solute strengthening, the twin nucleation strength is the sum of the stress to overcome the formation of the twin faults plus the solute strengthening contribution. If the solute/twin-boundary and solute/stacking fault interaction energies are not significantly different, then the motion of the partial dislocations (Fig. 1a,b) is identical to that modeled here (Fig. 1c). For NiCoCr, the $E_{n,twin}$ are fairly small (see Fig. 3a,b,c) and so the solid-solution strengthening for twin nucleation should be essentially the same as that for twin growth. The total twin nucleation strengths for the possible nucleation models are thus predicted to be

$$\tau_{t,nuc} = 89 \text{ MPa} \quad (\text{Atomistic} + \text{Mahajan}) \quad (10a)$$

$$\tau_{t,nuc} = 114 \text{ MPa} \quad (\text{Atomistic} + \text{Rao}) \quad (10b)$$

$$\tau_{t,nuc} = 107 \text{ MPa} \quad (\text{Elastic} + \text{Mahajan}) \quad (10c)$$

$$\tau_{t,nuc} = 135 \text{ MPa} \quad (\text{Elastic} + \text{Rao}) \quad (10d)$$

Examining the experiments, Uzer et al. [15] reported 78 ± 5 MPa from single crystal experiments. However, the origin of this value is unclear. Uzer et al. report (i) the approximate strains at which twinning is observed to begin as 4% for the [110] and 10% for the [111] and [123] orientations, (ii) the Schmid factors, and (iii) the stress-strain curves. From this information, we extract the twinning stresses for each orientation as shown in Fig. 5 and ranging from 72 MPa to 123 MPa. The predicted results for twinning controlled by nucleation are also shown in Fig. 5 using the elasticity model and the atomistic model. The predicted values are higher than the twinning stresses for [110] and [123] but comparable to or

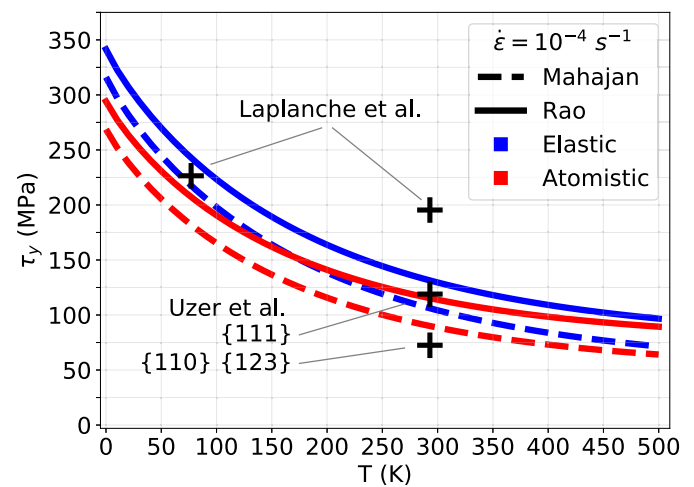


Fig. 5. Twin nucleation stress as predicted by the nucleation models of Rao and Mahajan (Eq. (1b) with $n = 2, 3$, respectively) and obtained using elasticity and atomistic inputs. Also shown are various experimental results as discussed in the main text.

lower than that for [111]. The Rao nucleus can also be augmented by impingement of a lattice dislocation to create a 3-layer twin that then grows at the same stress as the Mahajan nucleus, and so the lower values of the Mahajan nucleus (89–107 MPa) may be quantitative more consistent with experiments. Motion of a single partial dislocation with a trailing stacking fault is predicted to require much higher stresses of $\tau_p = 190 - 208$ MPa, indicating that growth does not occur by the initial creation of single stacking faults. Broadly, our analysis points toward twin nucleation as the controlling process, and the required stress is in the range of experiments.

Laplanche et al. [16] reported much higher estimates of the twinning stress in polycrystals. We revise their estimate by first extrapolating the yield strengths to the infinite-grain-size limit using the aggregated Hall-Petch data shown in Yin et al. [29], which shows the Hall-Petch contribution to strengthening to be 142 MPa. The backstresses caused by grain size effects should apply to twinning as well as bulk plastic flow, and so we subtract this strengthening from the reported twinning stress. Similar to Laplanche et al., we then use the Taylor Factor of 3.06 to estimate the critical resolved shear stress for twinning at both $T=77\text{K}$ and $T=293\text{K}$. The resulting twinning strengths are shown in Fig. 5.

Our predictions at T=77K for twin nucleation agree very well with the re-analyzed results from Laplanche et al. However, the experiments at T=293K are far higher than our predictions, and are also far higher than any of the single-crystal results from Uzer et al. The differences between the experiments of Uzer et al. and Laplanche et al. at T=293K requires resolution; the theory obviously cannot predict both results. However, the theory for twin nucleation (nucleation stress plus solute-strengthening stress to grow the nucleus) is in reasonable agreement with experiments of Uzer et al. at T=293K, suggesting that the single-crystal experiments are more quantitative.

4. Discussion

Here, we first seek some simplifications to provide insight into lattice dislocation versus twin dislocation strengthening for general alloys. To do so, we first neglect alloy-specific solute/twin boundary interactions so that twin strengthening is only controlled by the twin dislocation pressure field. In this limit, the key energy quantity Eq. (4) can be written as

$$\Delta \tilde{E}_p(w) = \left[\left(\sum_n c_n \Delta V_n^2 \right) \left(\sum_{i,j} \Delta p_{ij}^2(w) \right) \right]^{1/2} \quad (11)$$

where $\Delta p_{ij}(w) = p(x_i - w, y_j) - p(x_i, y_j)$. The pressure field due to an edge partial dislocation scales with b_p and the alloy elastic constants. For anisotropic materials, the Voigt-averaged elastic constants (μ^V, ν^V) give good agreement with full anisotropic models (see [30]), and hence the pressure field can be written as

$$p(x_i, y_j) = -\frac{\mu^V (1 + \nu^V)}{3\pi (1 - \nu^V)} f^t(x_i, y_j) \quad (12)$$

where $f^t(x_i, y_j)$ is a normalized pressure field of the twin. The minimization to obtain w_c^t for the twin then depends only on $\Delta f_{ij}^t(w) = f^t(x_i - w, y_j) - f^t(x_i, y_j)$, independent of the solute misfit volumes. If the structure of the twin dislocation is the same across fcc alloys, then $\Delta f_{ij}^t(w)$, w_c^t and $\Delta f^t(w_c^t) = \sum_{i,j} \Delta f_{ij}^t(w_c^t)$ are also the same across all fcc alloys. The strength of a lattice dislocation has exactly the same form but, due to the difference in dislocation structure as compared to the twin dislocation, with other values of w_c and $\Delta f(w_c)$ and the full lattice Burgers vector b . Therefore, the ratios of T=0 K strength and energy barrier for the twin (Eqs. (6) and (7)) to those for the lattice quantities can be written as

$$\frac{\Delta E_b^t}{\Delta E_b^l} = \left[\left(\frac{g^t(w_c^t)}{g^l(w_c^l)} \right)^2 \left(\frac{w_c^t}{w_c^l} \right)^2 \left(\frac{b_p}{b} \right)^1 \right]^{1/3} \quad (13)$$

$$\frac{\tau_{y0}^t}{\tau_{y0}^l} = \left[\left(\frac{g^t(w_c^t)}{g^l(w_c^l)} \right)^4 \left(\frac{w_c^t}{w_c^l} \right)^{-5} \left(\frac{b_p}{b} \right)^{-7} \right]^{1/3} \quad (14)$$

where the superscripts t and l stand for twin and lattice and $g(w_c) = [\sum_{i,j} \Delta f_{ij}(w_c)^2]^{1/2}$ is a dimensionless pressure field factor. We find $g^t(w_c^t) = 0.14$ and $w_c^t = 6b_p$ from the twin theory above while $g^l(w_c^l) = 0.32$ and $w_c^l = 9b_p$ are obtained from the lattice theory in Ref. [30]. The ratio of Burgers vector magnitudes in the fcc crystal is always $b_p/b = 0.577$. Therefore, we predict that the ratios of the energy barriers and zero-temperature stresses for twin dislocation glide versus lattice dislocation glide are then 0.37 and 2.36, respectively. *These ratios are constant independent of alloy composition if the solute/twin boundary interaction energies are negligible.* The zero-temperature twin strength is then notably higher than the lattice strength but the energy barrier is much lower.

Hence, the difference between twin and lattice strengths is a function of temperature and strain rate. Using the above ratios, we can further manipulate Eq. (8) as

$$\tau_y^t(T, \dot{\epsilon}) = [2.36\tau_{y0}^l] \exp \left[-\frac{1}{0.55} \left(\frac{kT}{[0.37\Delta E_b^l]} \ln \frac{\dot{\epsilon}_0}{\dot{\epsilon}} \right)^{0.91} \right] \quad (15)$$

Hence, the stresses required to move twin and lattice dislocations are then related as

$$\tau_y^t(T, \dot{\epsilon}) = 2.36\tau_y^l(2.7T, \dot{\epsilon}), \quad (16)$$

In words, the twin strength at temperature T is 2.36 times larger than the lattice strength at the higher temperature of 2.7T. For a given alloy, temperature-dependent bulk flow data can then be used to estimate the twin growth stress. The twin nucleation stress can further be estimated by adding the additional nucleation contribution (Eq. (1b)).

Recent work shows that the addition of Al and Ti to NiCoCr suppresses twinning [8]. One clear mechanism is simply due to a possible increase in stacking fault energy of the alloy. The present theory indicates also that increasing strength due to the addition of Al or Ti solutes could increase the difference between twinning nucleation stress and lattice strength. Neglecting changes in elastic properties at dilute concentrations of substitutional Al and neglecting solute/twin-boundary interactions, the solute strengthening of NiCoCrAl_x can be estimated by using the Al misfit volume $\Delta V_{Al} = 14 \text{ \AA}^3$ found previously for CoCrFeNi [31] as an additional contribution to the misfit term in Eq. (11). This increases the difference in twin versus lattice strength at T=300K, however the effect is only a few MPa. If the Al solutes have a larger interaction with the twin boundary than Ni, Co, or Cr, then the twin strengthening will be further increased, contributing again to suppression of twinning. Computation of the Al and Ti interactions with a twin boundary in NiCoCr or in elemental Ni are needed to make quantitative assessments.

More generally, if solutes in the alloy interact significantly with the twin boundary, i.e. if the $E_{n,twin}$ are large enough, then twin strengthening is increased. We examine the effects of $E_{n,twin}$ parametrically in a model system as follows. Using the NiCoCr twin pressure field, we artificially increase the $E_{n,twin}$ values for Ni, Co, and Cr from their initial values (-3.19, -2.74, 6.44 meV) by factors of 2. The values of E_{twin} for the two atoms on each side of the slip plane in the twin core are decreased to 2/3 and 1/3 of these values to give a smooth increase to zero in each plane of the twin structure. With these values, we compute ΔE_b and τ_{y0} for each case. Increases of $E_{n,twin}$ by factors of 2, 4, and 8 increase τ_{y0} and ΔE_b by (4.8% and 2.3%), (21.6% and 10.3%), and (76.4% and 32.8%) respectively. For the factor of 8 increase, the increased strengthening is quite significant while the solute/twin energies are still in the range 21–52 meV that is moderate for solute/fault interactions in other materials systems. These increases would suppress twinning relative to lattice dislocation motion. A quantitative understanding of solute/twin-boundary interactions is thus broadly important for accurate assessment of twinning strength.

Finally, the study here was executed for the edge partial dislocation since it is expected to have the highest strength and thus to control expansion of a twin dislocation loop or extended segment. A similar analysis can be performed for motion of the mixed 30° partial often studied as well. However, the screw component localizes the interaction energy more highly to the core. Results using atomistic inputs then deviate more significantly from those using the elasticity inputs, and the equilibrium distances w_c are smaller. Thus, "core" effects become more important but are quantitatively much less reliable, and so we show no results here [19,25,32,33].

5. Summary

The stress required to move a twin dislocation in a random alloy has been studied using solute strengthening theory and applied to the NiCoCr medium entropy alloy. Both elastic and atomistic inputs were used to estimate twin strengthening versus temperature. The twin growth stress is lower than experiments, indicating that twinning is controlled by nucleation. The theory was then extended to include existing nucleation models, and comparisons with available (and conflicting) experiments show reasonable results. Neglecting explicit solute/twin boundary interactions enables a direct comparison of twin strengthening versus bulk (lattice dislocation) strengthening. A parametric study shows the effects of solute/twin boundary interactions on the twin strengthening. The theory shows how twinning might be suppressed by the addition of dilute solute additions. Overall, the present work provides a theoretical framework for understanding the contributions of solute strengthening to the various processes associated with twin nucleation and growth in complex alloys.

Declaration of Competing Interest

The authors declare that they have no known competing financial interests or personal relationships that could have appeared to influence the work reported in this paper.

CRediT authorship contribution statement

R.E. Kubilay: Investigation, Formal analysis, Writing – original draft. **W.A. Curtin:** Conceptualization, Methodology, Supervision, Writing – original draft.

Acknowledgments

The authors thank Prof. Maryam Ghazisaeidi of the Ohio State University for useful comments and discussion, especially for driving a focus on the edge twin partial dislocations. The authors acknowledge support for this work by the Swiss National Science Foundation for the project #200021_181987 entitled “Harnessing atomic-scale randomness: design and optimization of mechanical performance in High Entropy Alloys”.

References

- [1] D.B. Miracle, O.N. Senkov, A critical review of high entropy alloys and related concepts, *Acta Mater.* 122 (2017) 448–511.
- [2] E.P. George, D. Raabe, R.O. Ritchie, High-entropy alloys, *Nat. Rev. Mater.* 4 (8) (2019) 515–534.
- [3] B. Gludovatz, A. Hohenwarter, D. Catoor, E.H. Chang, E.P. George, R.O. Ritchie, A fracture-resistant high-entropy alloy for cryogenic applications, *Science* 345 (6201) (2014) 1153–1158.
- [4] F. Otto, A. Dlouhý, C. Somsen, H. Bei, G. Eggeler, E.P. George, The influences of temperature and microstructure on the tensile properties of a CoCrFeMnNi high-entropy alloy, *Acta Mater.* 61 (15) (2013) 5743–5755.
- [5] A. Gali, E.P. George, Tensile properties of high-and medium-entropy alloys, *Intermetallics* 39 (2013) 74–78.
- [6] C. Varvenne, A. Luque, W.A. Curtin, Theory of strengthening in fcc high entropy alloys, *Acta Mater.* 118 (2016) 164–176.
- [7] S.S. Sohn, A. da Silva, Y. Ikeda, F. Körmann, W. Lu, W.S. Choi, B. Gault, D. Ponge, J. Neugebauer, D. Raabe, Ultrastrong medium-entropy single-phase alloys designed via severe lattice distortion, *Adv. Mater.* 31 (2019) 1807142.
- [8] C.E. Slone, C.R. LaRosa, C.H. Zenk, E.P. George, M. Ghazisaeidi, M.J. Mills, Deactivating deformation twinning in medium-entropy CrCoNi with small additions of aluminum and titanium, *Scr. Mater.* 178 (2020) 295–300.
- [9] S. Rao, TMS meeting presentation, 2019.
- [10] S. Mahajan, G.Y. Chin, Formation of deformation twins in fcc crystals, *Acta Metall.* 21 (1973) 1353–1363.
- [11] M. Ghazisaeidi, L.G. Hector Jr., W.A. Curtin, Solute strengthening of twinning dislocations in Mg alloys, *Acta Mater.* 80 (2014) 278–287.
- [12] Z.-H. Jin, P. Gumbsch, E. Ma, K. Albe, K. Lu, H. Hahn, H. Gleiter, The interaction mechanism of screw dislocations with coherent twin boundaries in different face-centred cubic metals, *Scr. Mater.* 54 (2006) 1163–1168.
- [13] M.P. Dewald, W.A. Curtin, Multiscale modelling of dislocation/grain boundary interactions. II. Screw dislocations impinging on tilt boundaries in Al, *Philos. Mag.* 87 (2007) 4615–4641.
- [14] A. Stukowski, Visualization and analysis of atomistic simulation data with OVITO—the open visualization tool, *Modell. Simul. Mater. Sci. Eng.* 18 (1) (2009) 015012.
- [15] B. Uzer, S. Picak, J. Liu, T. Jozaghi, D. Canadinc, I. Karaman, Y.I. Chumlyakov, I. Kireeva, On the mechanical response and microstructure evolution of NiCoCr single crystalline medium entropy alloys, *Mater. Res. Lett.* 6 (2018) 442–449.
- [16] G. Laplanche, A. Kostka, C. Reinhard, J. Hunfeld, G. Eggeler, E.P. George, Reasons for the superior mechanical properties of medium-entropy CrCoNi compared to high-entropy CrMnFeCoNi, *Acta Mater.* 128 (2017) 292–303.
- [17] B. Yin, W.A. Curtin, Origin of high strength in the CoCrFeNiPd high-entropy alloy, *Mater. Res. Lett.* 8 (2020) 209–215.
- [18] B. Yin, W.A. Curtin, First-principles-based prediction of yield strength in the RhIrPdPtNiCu high-entropy alloy, *npj Comput. Mater.* 5 (2019) 1–7.
- [19] C. Varvenne, G.P.M. Leyson, M. Ghazisaeidi, W.A. Curtin, Solute strengthening in random alloys, *Acta Mater.* 124 (2017) 660–683.
- [20] C. Varvenne, A. Luque, W.G. Nöhning, W.A. Curtin, Average-atom interatomic potential for random alloys, *Phys. Rev. B* 93 (10) (2016) 104201.
- [21] Q.-J. Li, H. Sheng, E. Ma, Strengthening in multi-principal element alloys with local-chemical-order roughened dislocation pathways, *Nat. Commun.* 10 (2019) 1–11.
- [22] S. Plimpton, Fast parallel algorithms for short-range molecular dynamics, *J. Comput. Phys.* 117 (1) (1995) 1–19.
- [23] U.F. Kocks, A.S. Argon, M.F. Ashby, Thermodynamics and kinetics of slip, *Prog. Mater. Sci.* 19 (1975).
- [24] A. Argon, *Strengthening Mechanisms in Crystal Plasticity*, vol. 4, Oxford University Press on Demand, 2008.
- [25] G.P.M. Leyson, L.G. Hector Jr., W.A. Curtin, Solute strengthening from first principles and application to aluminum alloys, *Acta Mater.* 60 (2012) 3873–3884.
- [26] G.P.M. Leyson, W.A. Curtin, Solute strengthening at high temperatures, *Modell. Simul. Mater. Sci. Eng.* 24 (2016) 65005.
- [27] F. Maresca, W.A. Curtin, Mechanistic origin of high strength in refractory BCC high entropy alloys up to 1900K, *Acta Mater.* 182 (2020) 235–249.
- [28] G.P.M. Leyson, W.A. Curtin, L.G. Hector, C.F. Woodward, Quantitative prediction of solute strengthening in aluminium alloys, *Nat. Mater.* 9 (2010) 750–755.
- [29] B. Yin, S. Yoshida, N. Tsuji, W.A. Curtin, Yield strength and misfit volumes of NiCoCr and implications for short-range-order, *Nat. Commun.* 11 (2020) 1–7.
- [30] S. Nag, C. Varvenne, W.A. Curtin, Solute-strengthening in elastically anisotropic fcc alloys, *Modell. Simul. Mater. Sci. Eng.* 28 (2020) 25007, doi:10.1088/1361-651x/ab60e0.
- [31] C. Varvenne, W.A. Curtin, Strengthening of high entropy alloys by dilute solute additions: CoCrFeNiAlx and CoCrFeNiMnAlx alloys, *Scr. Mater.* 138 (2017) 92–95.
- [32] L. Ventelon, B. Lüthi, E. Clouet, L. Proville, B. Legrand, D. Rodney, F. Willaime, Dislocation core reconstruction induced by carbon segregation in BCC iron, *Phys. Rev. B* 91 (22) (2015) 220102.
- [33] J.A. Yasi, L.G. Hector Jr., D.R. Trinkle, First-principles data for solid-solution strengthening of magnesium: from geometry and chemistry to properties, *Acta Mater.* 58 (17) (2010) 5704–5713.